Constructing 3D facial hierarchical structure based on surface measurements

Article *in* Multimedia Tools and Applications · November 2018

DOI: 10.1007/s11042-018-6839-y

CITATIONS
0

READS
39

4 authors:

Lv Chenlei
Nanyang Technological University
14 PUBLICATIONS **8** CITATIONS
SEE PROFILE

zk wu
Beijing Normal University
162 PUBLICATIONS **732** CITATIONS
SEE PROFILE

Xingce Wang
Beijing Normal University
58 PUBLICATIONS **199** CITATIONS
SEE PROFILE

Mingquan Zhou
Beijing Normal University
219 PUBLICATIONS **955** CITATIONS
SEE PROFILE

Multimedia Tools and Applications
https://doi.org/10.1007/s11042-018-6839-y

Constructing 3D facial hierarchical structure based on surface measurements

Chenlei Lv[1,2] · Zhongke Wu[1,2] · Xingce Wang[1,2] · Mingquan Zhou[1,2]

Received: 26 February 2018 / Revised: 22 August 2018 / Accepted: 5 November 2018 /
Published online: 15 November 2018

Abstract
In this paper, we propose a novel framework for 3D facial similarity measures and facial data organization. The 3D facial similarity measures of our method are based on iso-geodesic stripes and conformal parameterization. Using the conformal parameterization, the 3D facial surface can be mapped into a 2D domain and the iso-geodesic stripes of the face can be measured. The measure results can be regarded as the similarity of faces, which is robust to head poses and facial expressions. Based on the measure result, a hierarchical structure of faces can be constructed, which is used to organize different faces. The structure can be utilized to accelerate the face searching speed in a large database. In experiment, we construct the hierarchical structures from two public facial databases: Gavab and Texas3D. The searching speed based on the structure can be increased by 4-6 times without accuracy loss of recognition.

Keywords 3D facial hierarchical structures · Conformal parametrization · Facial data organization

1 Introduction

Biometric analysis is an important topic which attracts more attention to researchers. As a branch of biometric analysis, human faces analysis has been researched for many years and employed in many applications such as facial plastic surgery, craniofacial reconstruction, criminal investigations and security identification. Traditional works for face analysis

✉ Xingce Wang
wangxingce@bnu.edu.cn

[1] College of Information Science and Technology, Beijing Normal University, Beijing 100875, China

[2] Engineering Research Center of Virtual Reality and Applications, Ministry of Education, Beijing Key Laboratory of Digital Preservation and Virtual Reality for Cultural Heritage, Beijing Normal University, Beijing 100875, China

are mostly based on 2D facial images to extract facial features and construct analysis framework. The facial images are convenient to be obtained from the internet or simple data acquisition equipment directly. However, the performance of face analysis frameworks based on the facial images is affected by many factors such as facial expressions, light conditions, head poses, hair occlusions, cosmetics and blur in images. Such frameworks require complex pre-process to extract facial features of images. Because of the lack of complete geometric information, the accurate quantitative analysis such as the similarity measure for face data in image cannot be achieved from such frameworks basically. Based on such problems, some researchers attempt to construct facial analysis framework based on 3D scanning data.

The new technologies of 3D data scanning and 3D shape analysis are developing fast in recent years [34]. Comparing the traditional 3D scanning methods, the new scanning method does not require complexity devices with strict conditions. 3D scanning facial data have sufficient geometric information that can be used to support accurate quantitative facial analysis. The geometric information in a 3D scene is unaffected by lighting, cosmetics and other texture influence. Using new 3D data acquisition equipment, the geometric surface of the human face is acquired without natural noise. However, 3D facial data in applications of face analysis also be affected by some factors such as facial expressions and different kinds of occlusions. The mesh representation of 3D facial data is affected by different scanning devices, scanning distance and different people. 3D facial data are influenced by the accuracy of the triangulation meshes. 3D facial data for single person use more storage space and more computation for one process such as face recognition or facial similarity measures. Therefore, it is important to organize the 3D facial data from a large facial database for face analysis applications.

Based on the above considerations, we propose a 3D facial hierarchical structure construction framework, which can be used for 3D facial similarity measures and facial data organization. The framework includes the following two primary steps: constructing 2D facial area distortion representation and constructing the facial hierarchical structure. First, constructing 2D facial area distortion representation includes 3D facial data pre-processing, 2D facial reflection mapping and 2D facial area distortion representation construction. The pre-processing of the 3D facial data repairs the facial surface mesh, detects key landmarks and achieves iso-geodesic stripes. 2D facial reflection mapping transfers the 3D facial surface to a 2D facial reflection using conformal parameterization, while the 2D facial reflection preserves the main geometric information. 2D facial area distortion representation construction combines the 2D facial reflection and area distortion information into a facial data input for the next operation. Second, constructing the facial hierarchical structure includes 2D facial area distortion representation measurements and facial hierarchical structure building. We measure 2D facial area distortion representations using a measurement method called Discrete 2D Weighted Walkthroughs (D2DWW), and we achieve a distance matrix from a large facial database. Using the distance matrix, we can build a facial hierarchical structure that can be regarded as the 3D facial organization. In Fig. 1, we illustrate our framework.

In summary, the specific contributions of our work are as follows:

1) We propose a pipeline to construct facial organization from a facial database. The facial organization is a hierarchical structure. The structure can improve facial data searching speed in a large facial database.
2) We propose a facial similarity measure method called Discrete 2D Weighted Walkthroughs for 3D facial data. In our framework, the measurement method constructs a

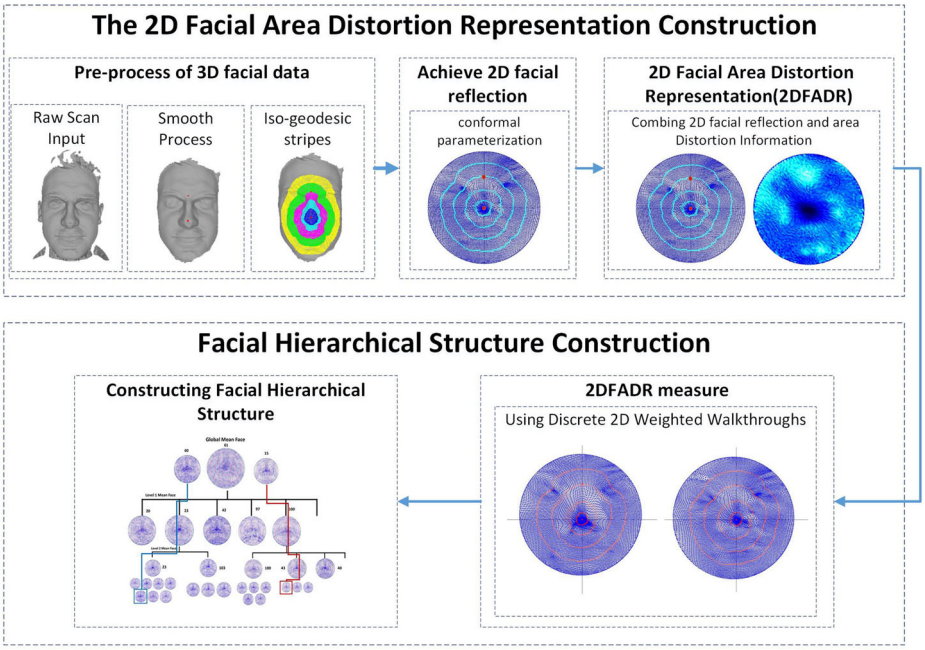

Fig. 1 3D facial data organization framework. The framework includes two steps: constructing the 2D facial area distortion representation and constructing the facial hierarchical structure. The 2D facial area distortion representation can be regarded as the input to construct the facial hierarchical structure

distance matrix from a large facial database. The matrix is used in facial organization construction. The measurement method is mathematical metric and robust to different facial expressions and triangulation accuracy.

3) We propose 2D facial area distortion representation using conformal parameterization. We use 2D facial reflections from 3D facial data and keep the area distortion. The 2D facial area distortion representation is regarded as the input for the measurement method and achieves the distance matrix. The head pose in the representation can be removed conveniently.

The remainder of our paper is organized as follows. In Section 2, we introduce some related works. In Section 3, we discuss the 2D facial area distortion representation construction. In Section 4, we illustrate facial hierarchical structure construction. The public facial databases, Gavab 3D and Texas 3D, were used in our experiment and are discussed in Section 5.

Explanation for some important items of equations:

$C_A, C_B, C_1, C_2, C_1', C_2'$: iso-geodesic stripe.

$\omega_{i,j}(C_A, C_B)$: the weight code of two stripes from certain direction (i, j).

$\omega(\mathrm{C_A}, \mathrm{C_B})$: the weight code of two stripes from all directions.

F, F': facial surface with different iso-geodesic stripes

$D_s(F, F')$: D2DWW for facial surfaces (just two stripes in one surface are selected which can be regarded as a local measure result).

$D_g(F, F')$: D2DWW for facial surfaces (all stripes in one surface are selected which can be regarded as a global measure result).

2 Related works

The 3D facial hierarchical structure construction framework includes facial similarity measures and facial data organization. Facial measures is used to compute the similarity or distance between different faces. Facial organization combines the information on facial similarity result to build a global structure of a large facial database. We discuss the related works based on the two parts.

For facial similarity measures, the iso-geodesic curves and surface parameterization have been widely used in such applications. Berretti [5, 6] proposed a method that used iso-geodesic stripes and 3D weighted walkthroughs to achieve face matching results. Jahanbin [22] proposed a face recognition method based on iso-geodesic curves and iso-depth curves. He attempted to improve the recognition accurate by Procrustes Analysis [23], which was used to remove the influence of head pose. Ahdid [1] combined the iso-geodesic curves and space reduction methods (Principal Component Analysis & Fisher Linear Discriminant Analysis) to construct an automatic 3D face recognition system. Fakir [16] proposed a iso-geodesic curves based method for 2D face recognition system, which was constructed in a Riemannian framework.

Some methods were based on facial surface parameterization theory. Bronstein [9, 10] constructed a canonical form for a 3D face to remove the facial expression effects. Xia [39, 40] proposed an expression invariant method for compressing geometric information. Zeng [42, 43] and [44] applied Ricci flow theory and a series of parametric methods to map 3D facial data to a parameter domain. Anuj introduced a square-root velocity (SRV) [36] method to compare the shape similarity of different curves. To measure facial similarity, the authors searched geodesic circles in a 3D facial surface and compared the circles in the shape space [15]. Jermyn [24] extended the idea to a surface matching problem and Kurtek [25] used the related theory in 3D facial analysis. Such measurement methods consider the facial expressions' influence in facial measurement. However, the measurement results are affected by differing triangulation mesh accuracy. Some measurement methods are not strictly mathematically metric.

For facial organization, there have two ways to construct the facial subclasses or structure: classification based and clustering based. The classification based methods divided the facial data based on facial attributes such as gender and race. Lyons [28] proposed a linear discriminant analysis model to different classification tasks. Horng [21] proposed an age classification method based on facial features. Wu [38] constructed a statistical model from 2.5D facial needle-maps to classify human gender. Ballihi [3] extracted radial curves and iso-level curves to represent 3D facial shapes and achieve gender classification. Facial classification divides the facial data into certain classes based on prior information. Using the facial classification results, we cannot build an accurate facial organization with various subclasses.

Facial clustering based methods divided facial data based on quantitative property such as age, expressions and facial similarity. Choi [12] combined hybrid features and a hierarchical classifier to estimate human age from a facial image. Antipov [2] proposed an age estimation method using a certain convolutional neural network (CNN). Ghahari [19] proposed an automatic facial expression analysis system using a canny edge detector. Lopes [26] used a convolutional neural network to recognize a facial expression from images. Li [17] proposed a facial clustering method based on facial similarity. Using the facial clustering results,

we can achieve accurate facial organization. However, most facial clustering methods are based on 2D facial images. The clustering results are dependent on facial databases and label information. It is difficult to build an accurate evaluation for the clustering result. This difficulty is observed because the facial images do not have a regular form and the distance between facial data from different classes are not mathematically metric.

Based on the facial clustering results, some researchers proposed the facial organization framework. Li [12, 17] proposed a Hierarchical Agglomerative Clustering (HAC) from the facial clustering method that can be regarded as facial organization. Drira [15] proposed a facial hierarchical structure based on 3D nose similarity. The face modeling method is another solution for facial structure construction. Blanz proposed a Morphable Model [7] to synthesize 3D faces in facial spaces. In [8], the author proved that the Morphable Model has great face recognition capabilities. Many works follow with similar ideas [11, 33]. Such a facial data organization method can build a facial organization structure to a large facial database. However, facial organization performance is dependent on facial data quality. The facial organization process is not robust to different facial data accuracy, including 2D facial images and 3D facial surfaces. The Morphable Model can provide a regular facial data representation, but it is deeply dependent on a face sample database. Using different face sample databases cannot achieve a stable Morphable Model. The feature vectors in a low dimensional facial space are not coincident with human perceptions.

Recently, deep learning algorithms were developing fast and the related tools were used in facial data analysis. Shan [35] used convolutional neural networks (CNN) to achieve real-time gender classification results from facial images. Yu [41] proposed a deep leaning network for face recognition. The network was an integration scheme which includes principal component analysis, support vector machine and extreme learning machine. Mühling [30] proposed a content-based video track system by deep learning approaches. The facial data in videos were tracked and clustered by identity information. Otto [31] proposed a face clustering method which was used to recognize the identity from a large facial database. Luciano [27] proposed a deep learning framework based on geodesic moment features for 3D shape classification. In another work [29], they attempted to improve the accurate of shape analysis based on spectral graph wavelets and the bag-of-features paradigm, which were used to capture the local and global geometric features. Basically, the face analysis by deep learning was focus on identity recognition. It was difficult to build a creditable framework for different faces clustering task. The similarity of faces from different persons was difficult to be achieved from facial images. For 3D facial data, the deep learning framework required the complex transfer to obtain regular input data. The pre-process increased the computation. Therefore the deep learning framework was not appropriate for our task.

In our framework, we propose facial data representation, 2D facial area distortion representations (2DFADR). The 2DFADR includes facial landmarks, 2D facial reflection, area distortion information and iso-geodesic stripes. The landmark detection method [20] is used to detect landmarks on 3D facial surfaces. The conformal parameterization method [14] is used to achieve 2D facial reflection and area distortion information. The iso-geodesic stripes in our framework are identical to [1]. To measure the 2DFADR, we propose the Discrete 2D Weighted Walkthroughs (D2DWW) method. The method is based on 2D Weighted Walkthroughs [4]. The difference between the two is the D2DWW considers the area distortion information of the 2DFADR in its respective measurement. In the facial organization

process, we use Affinity Propagation (AP) [18] iteratively in the distance matrix from the 2DFADR measurement results. A facial data hierarchical structure is achieved, and it can be regarded as the facial organization. In the following sections, we discuss the details of our framework.

3 2D facial area distortion representation for 3D face

In our framework, the 3D facial data should be transferred to regular form. It is necessary for the facial measurement process. We propose the facial regular form of the 2D facial area distortion representation (2DFADR). The 2DFADR combines the 2D facial reflection from a 3D facial surface by conformal parameterization and the area distortion information. In our work, the goal is to find a mapping of a 3D facial surface to a 2D facial reflection that preserves the main geometric features. Usually, the mapping would produce area distortion to the triangular meshes. To reduce the influence of the area distortion, an energy cost function for the distortion is proposed. The target of the mapping is to find the 2D reflection that preserves the main geometric features of the 3D object. In the following parts, we discuss the necessary pre-processing, the conformal parameterization method and the construction of 2DFADR.

3.1 Pre-processing of 3D facial data

The general pre-processing of the raw 3D facial data has been discussed in previous works [5, 39]. In this paper, we only discuss the processes that have relationships with conformal parameterization. First, we detect the facial landmarks in 3D facial data. Facial landmarks are needed for geometric feature extraction and facial alignment. In 3D face data, using shape analysis to detect special points is an enabling method discussed in recent research [20]. We apply this idea to achieve the nasal and eyebrow tip positions. We compute the geodesic of the two landmarks to define a confirm direction and normalized distance. The geodesic curves are achieved by [37]. By combining the landmarks with the direction and distance, we can achieve iso-geodesic stripes.

We use the iso-geodesic stripes to represent facial surface geometric features. In conformal parameterization, the stripes are mapped to a 2D reflection. There are different banding areas that satisfy specific geodesic distances from area points to the nasal tip. The banding areas are adjacent to each other and represent different facial regions. In (1), S is the facial surface and p is the point in S. Every point in S has a geodesic distance to the nasal tip p_{nose}. Using different geodesic distances, we can achieve different banding areas (Fig. 2). While some expressions change the topological structure of the facial surface (open mouth and close eyes), we do not consider such conditions.

$$c_n = \{p | p \in S, geodesicDis(p, p_{nose}) \in threshold(c_n)\} \tag{1}$$

3.2 Achieve 2D facial reflection by Conformal Parameterization

Conformal parameterization builds differential homeomorphisms between 3D surfaces and 2D reflections. The process preserves some intrinsic characteristics. Ideally, the conformal parameterization is isometric. In fact, it is impractical for 3D facial data. Gauss curvatures for each point in 3D facial data are not identical, which expresses the change of the first fundamental form. In our work, we use a conformal parameterization process for 3D facial

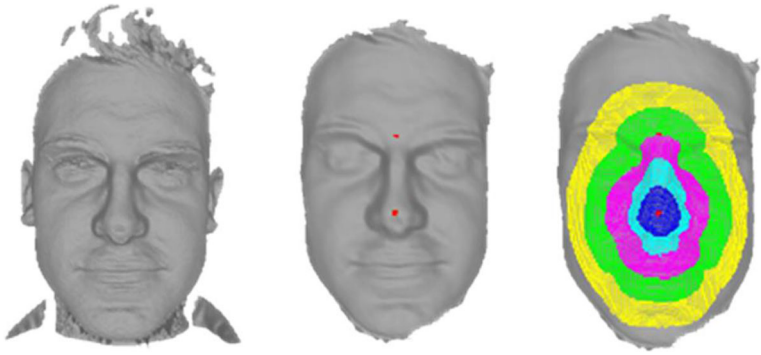

Fig. 2 The facial landmarks (nasal and eyebrow tips which are signed by red points) and the iso-geodesic stripes (different colors represent different stripes) in 3D face

data by optimizing two kinds of transfer energy: Dirichlet Energy E_A (2) and Chi Energy E_χ (3) [14].

$$E_A = \sum_{oriented\_edges(i,j)} \cot\alpha_{ij} \left|u_i - u_j\right|^2 \tag{2}$$

$$E_\chi = \sum_{j\in N(i)} \frac{(\cot\gamma_{ij} + \cot\delta_{ij})}{|x_i - x_j|^2}(u_i - u_j)^2 \tag{3}$$

x_i and x_j are points in the 3D facial surface, u_i and u_j are points in the 2D mapping result. $N(i)$ means the adjacent points of i and the angles α_{ij}, γ_{ij} and δ_{ij} are shown in Fig. 3. We achieve the conformal parameterization result by computing the extreme value from the two energy functions (4) and (5).

$$\frac{\partial E_A}{\partial u_i} = \sum_{j\in N(i)} (\cot\alpha_{ij} + \cot\beta_{ij})(u_i - u_j) = 0 \tag{4}$$

$$\frac{\partial E_\chi}{\partial u_i} = \sum_{j\in N(i)} \frac{(\cot\gamma_{ij} + \cot\delta_{ij})}{|x_i - x_j|^2}(u_i - u_j) = 0 \tag{5}$$

To compute the global optimization value from the conformal parameterization, the Linear Equation group is constructed. Equation (6) illustrates the Linear Equation group from

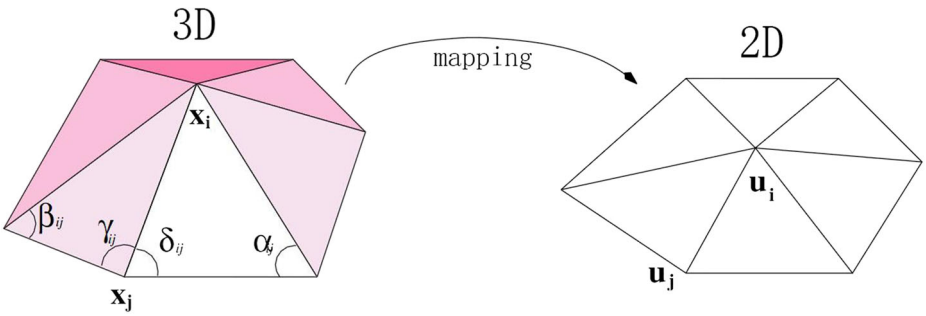

Fig. 3 Conformal parameterization from the 3D data to 2D reflection. The 3D meshes are mapped into 2D platform and the geometric features are retained

the global optimization of (4) and (5). In particular, the landmarks $U^{landmarks}$ and boundary points $U^{boundary}$ of the 3D facial surface are predefined in the 2D reflection. The 2D reflection is a 2D triangular mesh surrounded by facial boundary points. The triangular mesh constructs a circle, and the center is the nasal tip. The eyebrow tip is settled in a vertically upward direction in the circle. $C^{landmarks}$ and $C^{boundary}$ represent the coordinates of landmarks and facial boundaries in the 2D reflection. Therefore the 2D reflection of the 3D facial surface is a standard circle with two registration landmarks. In (6), the parameters λ and μ determine the weight of the two kinds of energy in the parameterization. Each item in the linear system can be computed by (7) and (8). We discuss the detail of the values in Section 4. In Fig. 4, we achieve the 2D reflection result with iso-geodesic stripes.

$$\begin{bmatrix} \lambda M^A + \mu M^\chi \\ 0\ I\ 0 \\ 0\ 0\ I \end{bmatrix} \begin{bmatrix} U^{internal} \\ U^{\text{landmarks}} \\ U^{\text{boundary}} \end{bmatrix} = \begin{bmatrix} 0 \\ C^{\text{landmarks}} \\ C^{\text{boundary}} \end{bmatrix} \tag{6}$$

$$M_{ij}^A = \begin{cases} \cot(\alpha_{ij}) + \cot(\beta_{ij}) & if\ j \in N(i) \\ -\sum_{k \in N(i)} M_{ik}^A & if\ i = j \\ 0 & otherwise \end{cases} \tag{7}$$

$$M_{ij}^\chi = \begin{cases} \cot(\gamma_{ij}) + \cot(\delta_{ij}) / \left| x_i - x_j \right|^2 & if\ j \in N(i) \\ -\sum_{k \in N(i)} M_{ik}^\chi & if\ i = j \\ 0 & otherwise \end{cases} \tag{8}$$

3.3 2D Facial Area Distortion Representation (2DFADR)

By combining the 2D facial reflection result, we propose the 2DFADR. The 2DFADR is the 2D facial reflection with area distortion information. Area distortion is inevitable between a 3D facial surface and 2D reflection. In our framework, the area information of the iso-geodesic stripes is important. Area distortion influences the measurement result. Therefore, we use an area distortion representation to record the distortion. Using the representation, we can reduce the area distortion's influence in a measurement step. The 2DFADR is constructed by the area distortion parameter of every triangular mesh in the 2D reflec-

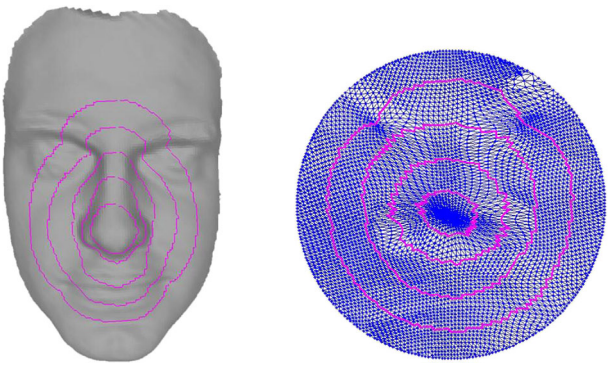

Fig. 4 2D facial reflection result of a 3D facial surface by conformal mapping. The borders (purple curves) of different iso-geodesic stripes are retained from 3D facial surface to 2D reflection.

tion. S_t is the 3D facial surface of the 3D triangular mesh. Here, $S_t = t_1, ..., t_k$, t_i is a triangle, and k is the number of triangles. S_{tc} is the 2D facial reflection of S_t, $S_{tc} = tc_1, ..., tc_k$ and tc_i is the 2D triangle. At is the area distortion representation, in which $At = \delta_1, ..., \delta_k, \delta_i = area(t_i)/area(tc_i)$. The parameters are computed by the original 3D triangle dividing the 2D reflection. In Fig. 5, we show an instance of area distortion representation. The color becomes deeper as the area distortion becomes more pronounced.

4 Facial hierarchical structure construction

In this part, we introduce the facial hierarchical structure construction. The construction includes two steps. First, we measure the 2DFADR of facial data. By combining the iso-geodesic stripes in the 2DFADR, we propose a novel measurement method called Discrete 2D Weighted Walkthroughs (D2DWW). Our measurement method considers the influence of area distortion. Second, we use the 2D reflection measurement results to build a facial hierarchical structure, using a suitable clustering algorithm and controlling the data number in a single node. The facial hierarchical structure can improve facial data searching and matching.

4.1 2DFADR measurement

Combining the 2DFADR and iso-geodesic stripes in the 2D facial reflection, we propose a facial surface measurement method, the Discrete 2D Weighted Walkthroughs (D2DWW). The D2DWW is based on the 2DWW [4], as it computes adjacent iso-geodesic stripes' relative positions in the 2D facial reflection to achieve measurement results. After conformal parameterization, the triangular meshes in 2D reflection are different to original meshes in 3D face. The 2DWW cannot be used to measure the 2DFADR directly. The D2DWW is proposed to correct the distortions of triangular mesh based on 2DFADR. The stripes in the D2DWW are represented by points. For the stripes' measurement, we first should illustrate points' relative positions in Fig. 6 and (9). $P_1(x_1, y_1)$ and $P_2(x_2, y_2)$ are the points in the stripes. In each axis, there are three conditions of the relative positions. On the horizontal axis, the three conditions are right, left and near. On the vertical axis, the three conditions are above, below and adjacent. The threshold determines which conditions of the points are

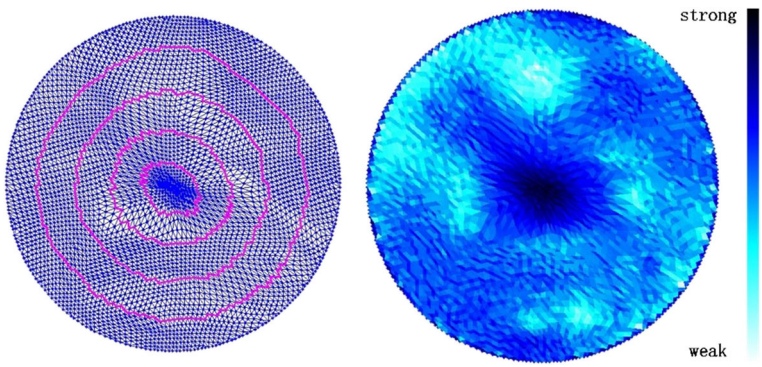

Fig. 5 Degree of area distortion in the 2DFADR. The left image is the 2D facial reflection from a 3D facial surface by conformal parameterization. The right image is the 2DFADR with area distortion color labeling

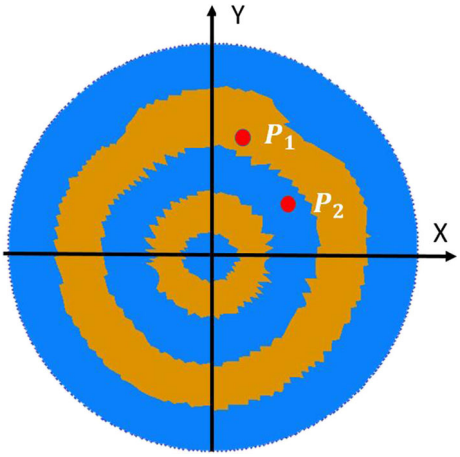

Fig. 6 The two points in the stripes. The different colors represents different stripes in 2D reflection. Using the (9) ($i = 1; j = -1$)

near. Using the appropriate threshold can reduce the influence of area change in conformal mapping.

$$i = \begin{cases} -1, & x_2 - x_1 < \text{ - threshold} \\ 0, & |x_2 - x_1| <= \text{threshold} \\ +1, & x_2 - x_1 > \text{threshold} \end{cases}, j = \begin{cases} -1, & y_2 - y_1 < \text{ - threshold} \\ 0, & |y_2 - y_1 — ¡ = \text{threshold} \\ +1, & y_2 - y_1 > \text{threshold} \end{cases} \quad (9)$$

$$w_{i,j}(C_A, C_B) = \frac{1}{N(C_A) * N(C_B)} * \int_{C_A} \int_{C_B} N_{ij}((x_a, y_a), (x_b, y_b)) dx_b dy_b dx_a dy_a \quad (10)$$

The stripes' relative positions are represented by the points. In (10), the weight code of the stripes' relative position (certain direction i, j) is proposed. C_A and C_B are two iso-geodesic stripes from one facial surface, A and B are indexes of the stripes. $N(C_A)$ and $N(C_B)$ indicate the density point numbers of the stripes C_A and C_B, respectively. The density point number is determined by the discrete area of the stripes. The detail algorithm is described as follows. First, we set a constant d to fix point numbers in C_A and C_B. Second, we assign the points to each triangle mesh according to an area ratio between the mesh and stripes. The areas of the mesh and stripes are corrected by an area distortion representation. Finally, we compute the point numbers of the stripes C_A and C_B. N_{ij} is the number of points' pairs that satisfy the encode condition (i, j). The process is based on density point numbers in a triangular mesh. In Fig. 7, we show an instance of the w_{ij} computation process.

Using (9) and (10), we achieve a 3*3 measurement matrix for two stripes. The w_{ij} of different directions should be multiplied by their corresponding parameter to represent different degrees of the distribution. In (11), we add the parameters to correct the measurement matrix.

$$w(C_A, C_B) = \begin{bmatrix} w_{-1,1} & \lambda_2 w_{0,1} & w_{1,1} \\ \lambda_1 w_{-1,0} & \lambda_0 w_{0,0} & \lambda_1 w_{1,0} \\ w_{-1,-1} & \lambda_2 w_{0,-1} & w_{1,-1} \end{bmatrix} = \begin{bmatrix} w_{-1,1} & w_{0,1} & w_{1,1} \\ w_{-1,0} & w_{0,0} & w_{1,0} \\ w_{-1,-1} & w_{0,-1} & w_{1,-1} \end{bmatrix}_{new} \quad (11)$$

$$\lambda_0 = \sqrt{N(C_A) \times N(C_B)}, \lambda_1 = \frac{N(C_A) \times N(C_B)}{L_B \times L_{AB} \times H_{AB}}, \lambda_2 = \frac{N(C_A) \times N(C_B)}{H_B \times L_{AB} \times H_{AB}}$$

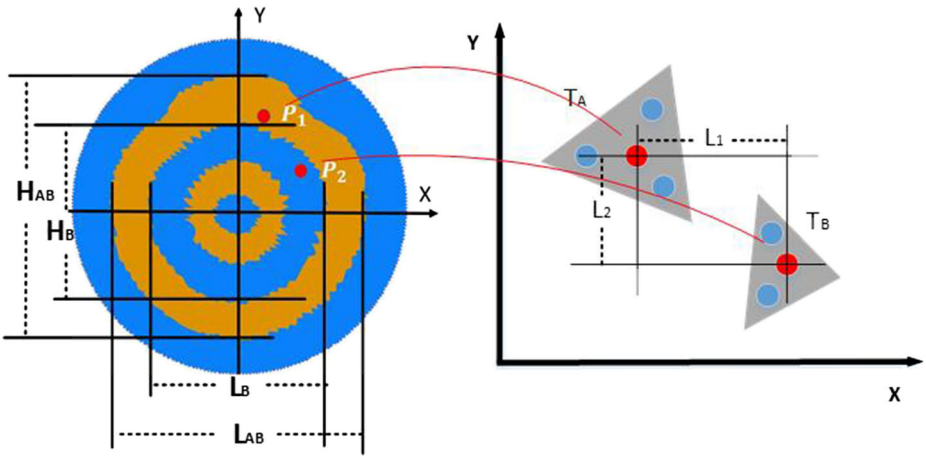

Fig. 7 Computation process instance of w_{ij}. T_A and T_B are triangular meshes from the stripes C_A and C_B. The blue points are density points. The red points are centers of the triangular meshes. The point pairs' number is six (3*2). We use the center point's relative position to represent the density points. $L_1 > L_2 > threshold$. $N(T_A) * N(T_B) = 6$. $N_{(1,-1)} = 6$, $w_{(1,-1)} = 1 . N_{ij} = 0$, $w_{ij} = 0 (i \neq 1, j \neq -1)$

By combining different w_{ij} from the different stripes in the 2DFADR, we achieve the surface measurement result. In (12), C_1 and C_2 are the stripes in face F, and C'_1 and C'_2 are the stripes in face F'. We achieve the similarity of F and F' by measuring the stripes.

$$D_s(F, F') = D_s(w(C_1, C_2), w(C'_1, C'_2)) \tag{12}$$

$$\begin{aligned} D_s(w, w') = {} & \lambda_H d_H(w, w') + \lambda_V d_V(w, w') \\ & + \lambda_D d_D(w, w') + \lambda_{H0} d_{H0}(w, w') \\ & + \lambda_{V0} d_{V0}(w, w') + \lambda_{00} d_{00}(w, w') \end{aligned} \tag{13}$$

$$\begin{aligned} d_H &= |(w_{1,1} + w_{1,-1}) - (w'_{1,1} + w'_{1,-1})|, \\ d_V &= |(w_{-1,1} + w_{1,1}) - (w'_{-1,1} + w'_{1,1})|, \\ d_D &= |(w_{-1,-1} + w_{1,1}) - (w'_{-1,-1} + w'_{1,1})|, \\ d_{V0} &= |(w_{-1,0} + w_{1,0}) - (w'_{-1,0} + w'_{1,0})|, \\ d_{H0} &= |(w_{0,-1} + w_{1,0}) - (w'_{0,-1} + w'_{0,1})|, \\ d_{00} &= |(w_{0,0}) - (w'_{0,0})| \end{aligned}$$

In fact, there are not only two iso-geodesic stripes in a face. Therefore we extend (12–14). The similarity measurement of (14) is mathematically metric. It is determined by (13). λ_{ij} means the weight of stripes C_i and C_j in the face similarity measurement. The index of the stripes i and j should be adjacent. The reason is that the adjacent stripes' relative positions are robust to facial expressions (15). ΔE indicates the change of the points in stripes by facial expressions.

$$\begin{aligned} F = (C_1, ...C_k), F' = (C'_1, ...C'_k) \\ D_g(F, F') = \sum_{\substack{i=0, j=0 \\ i \neq j, j-i=1}}^{k} \lambda_{ij} D(w(C_i, C_j), w(C'_i, C'_j)) \end{aligned} \tag{14}$$

$$w(C_i, C_j) \approx w(C_i + \Delta E, C_j + \Delta E), |i - j| \leq 1 \tag{15}$$

4.2 Constructing facial hierarchical structure

Our main goal is constructing an effective facial organization. In our framework, the organization is a facial hierarchical structure. The structure can be regarded as an effective organization for facial database. The structure can improve face recognition speed and clustering different faces by certain regulation. We extend the similar idea in global facial surface. For statistical analysis in the hierarchical structure, the "mean face" is useful. We compute the mean face which can be regarded as the center of the faces. In (16), first, the facial set S is defined. We use the (13) to represent the facial distances. Finally, we can achieve the mean face $\bar{F}$ of the set S in (17).

$$S = \{F_1, ...F_n\}, V(F_m) = \sum_{i=1}^{n} D(F_m, F_i) \tag{16}$$

$$\overline{F} = \arg \min_{F_m \in S} V(F_m) \tag{17}$$

The set S is not a continuous face space, therefore the mean face $\bar{F}$ is not a precise center of the set. However, the mean face represents aggregate trends of a facial set and provides a tool for building a hierarchy structure. In Fig. 8, we show the instance of the mean face.

Several clustering algorithms, such as K-means [13] and K-medoids [32], require users to provide the number of centers. It is difficult to provide reliable numbers of centers in a large facial database. To construct the facial hierarchical structure, we employ the classical clustering method Affinity Propagation (AP) [18]. The AP method is suitable for our facial structure building framework. We can achieve the clustering results using measurement results and do not need to set the number of the center. The mean face is the center in the subset. The facial distances are represented by our surface measurement results. We achieve the hierarchical structure by iterating the AP method. The number of data in a node can be controlled. When the number of data in a node is more than one threshold, we subsequently use the AP method to cluster the data into different classes. Using this method, we build a facial hierarchical structure. In Algorithm 1, we explain the details for hierarchical structure construction. In Fig. 9, we show the hierarchical structures for Texas3D and two instances

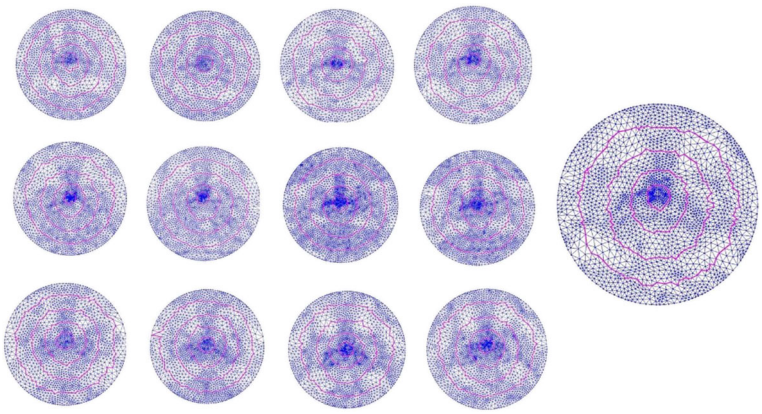

Fig. 8 Instances of 2D facial reflections. Right-side data are the mean face of 12 faces on the left

with search paths. The hierarchical structure sets up an effective facial structure. We would show the improvement by the structure in facial data searching works.

Algorithm 1 Facial hierarchical structure construction

Require: 2DFADR set of facial database $S\{F_1 ... F_n\}$.

Define the initial list H_s to store the hierarchical structure.
Define the level L_H.
Define the threshold T_S to limit the 2DFADR number in subclasses.
Initial $L_H = 0$.
function(S, H_s){
  if (2DFADR Number in $S <= T_S$){
    stop and jump out.
  }
  else{
    L_H++.
    $Ap(S) = \{S_i, ...S_k\}$
    for i to k\{
      $\overline{F}_i = Equation17(S_i)$.
      Add $\{\overline{F}_i, S_i, L_H\}$ into H_s.
      function(S_i, H_s).
    }
  }
}

Ensure: H_s

5 Experiments

There are two performance indexes to illustrate the effectiveness of our facial hierarchical structure construction method. First, we improve the facial search speed in a facial database. Using the facial hierarchical structure, the facial recognition or search process for a huge facial database can instead be a sample computation by several facial measurement processes. Second, we improve the accuracy of facial classification in this structure. In our facial hierarchical structure, the facial data is divided into different nodes regarded as facial classes. The classification process is robust to facial expressions and triangular meshes with different accuracies. We build test data sets in the public face databases Gavab and Texas 3D, which have been widely applied to facial recognition work. Facial data in the two facial databases have different facial expressions. In Gavab, every single person has nine samples with different head poses. In Texas 3D, the facial numbers and degrees of expressions are not standard for each person, but the faces are sampled with same head pose and have 25 landmarks. It includes 1149 scans from 116 persons. We use 3*61 samples from Gavab to build the structure and other samples to be the test set. We also use 2*116 samples from Texas3D to build the structure and other samples to be the test set. Some persons in Texas3D just have single sample. In structure construction process, we just copy the sample and keep the numbers in 2DFADR clustering process. In the following sections, we discuss our facial structure performance in detail by explaining the influence of some parameters configurations, showing the improvement of search speed using our facial structure and showing the facial classification accuracy of our facial structure.

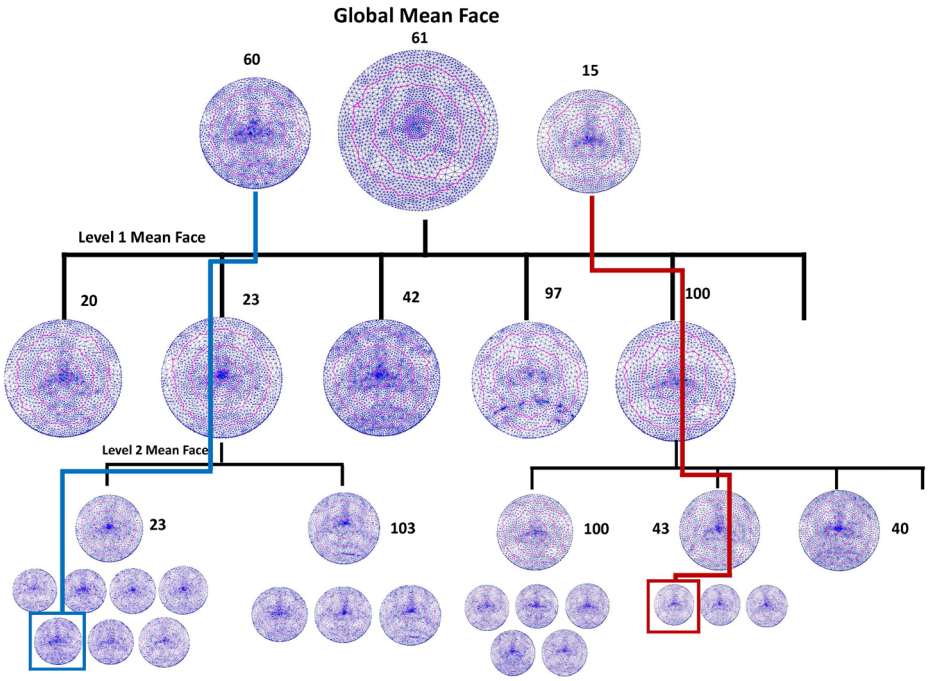

Fig. 9 Two search instances in hierarchical structure. The blue and red lines represent the searching path from source 2D facial reflections to target facial reflections. The facial reflection of mean face are stored in each level of the structure. Comparing the facial reflections of source face and mean face in different levels, the target face can be located

5.1 Parameter configuration

In our framework, some parameters influence the accuracy of the facial surface measurement method that determines the structure construction performance. The parameters are the weights of the two energies and the threshold in (6) and (9), the number of the iso-geodesic stripes and the weights in (14). In the conformal parameterization process, the two energies determine the triangles' change from a 3D facial surface to a 2D reflection. The Dirichlet Energy is sensitive to angle change, and the Chi Energy is sensitive to changing triangle length. In Fig. 10, we show the different conformal parameterization results with different weights for Dirichlet and Chi Energy. Increasing the weight of Dirichlet Energy induces area distortion. The opposite induces angle distortion.

We evaluate the performance with five conditions: $M1$(threshold = 0.01, Dirichlet: Chi = 1:0), $M2$ (threshold = 0.05, Dirichlet: Chi = 1:0), $M3$ (threshold = 0.01, Dirichlet: Chi = 1:1), $M4$ (threshold = 0.01, Dirichlet: Chi = 0:1) and $M5$ (threshold = 0.05, Dirichlet: Chi = 0:1). The receiver operating characteristic curve (ROC) result of facial recognition is computed from different facial databases in Fig. 11. Basically, the precision is better with a smaller threshold and worse with a higher weight of Chi energy. We achieve the data with four iso-geodesic stripes.

Naturally, different numbers of iso-geodesic stripes influence the performance of the method. The additional stripes can improve precision but will increase time complexity. In Table 1, the time cost of our method with different numbers of stripes in two facial databases

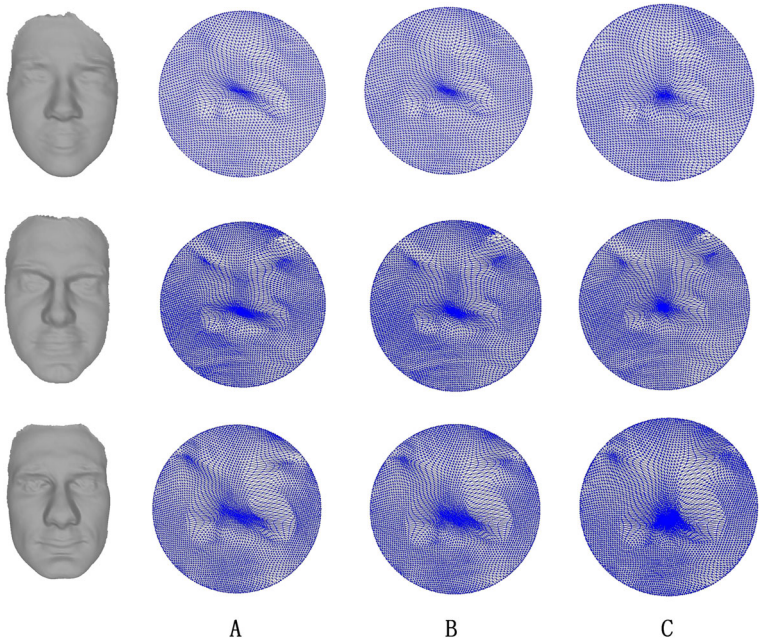

Fig. 10 The different conformal mapping results with different weights of two energies. (Dirichlet: Chi) $A = 0:1$, $B = 1:1$, $C = 1:0$

are proposed. When the number of stripes is greater than a certain quantity, precision improvement is not obvious. Two dense stripes increase the sensitivity to facial expressions. In contrast, insufficient quantity of stripes cannot address the requirement for facial similarity measurement. In Fig. 12, we also show the facial recognition ROC results in different databases with differing number of stripes ($S3 = 3$, $S4 = 4$, $S5 = 5$, $S6 = 6$, $S7 = 7$). For the weights of (13), we choose a set of values ($\lambda_V = 1/3, \lambda_V = \lambda_D = 1/4, \lambda_{V0} = \lambda_{H0} = 1/12$). For the weights of (14), the general way uses the learning framework, such as linear regression, to optimize a set of weights. We use the same weights in our frameworks since the weights from the learning methods may produce the locally optimal results. In certain

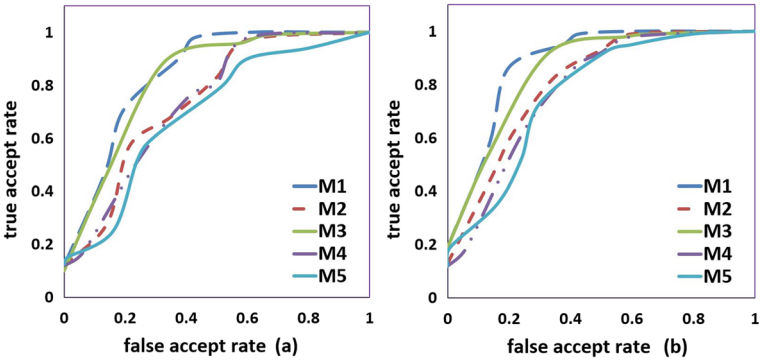

Fig. 11 ROC result with different thresholds and ratios(Dirichlet:Chi). **a**: Texas3D, **b**: Gavab

Table 1 Average time cost for face similarity measure for different facial databases with different stripes numbers

	Stripes number				
Facial database	3	4	5	6	7
Texas3D	5.3s	7.8s	9.3s	13.4s	18.6s
Gavab	6.1s	9.8s	12.4s	16.5s	24.3s

applications, the weights can be computed according to the actual situation. Finally, we set the parameters in our framework, which includes threshold (0.01), ratio of Dirichlet & Chi (1:0) and stripes (5).

5.2 Facial hierarchical structure for increasing facial search speed

We construct the hierarchical structure in Gavab to show the facial search speed improvement. The performance indexes are discussed to evaluate the facial structure. We first show the facial search speed improvement of our facial hierarchical structure. The surface measurement method is the determinant of hierarchical structure building. We use several surface measurement methods to build different facial hierarchical structures and compare the average search speed. 3DWW [5] is dependent on a coordinate system in R3 space. The measurement precision is influenced by facial alignment. Therefore, the method is not intrinsic. SRV [15] proposes a hierarchical structure using nose measurement in the shape space. We use the methods to construct different facial hierarchical structures. The facial data speed is different using different methods, under which the structure's measurement methods influence the speed. In Table 2, we show the average search speed using different methods over two facial databases. The Gavab test set includes 244 faces from 61 people. The Texas3D test set includes 200 faces from 100 people. The results show the improvement by the hierarchical structures. The 3DWW and our D2DWW are faster in the search process. The reason is that the methods compute the relative positions of the stripes. The results were achieved during the pre-processing. In facial searching, the measurement method compares the computed results. The structures have a clear improvement for the huge facial data test

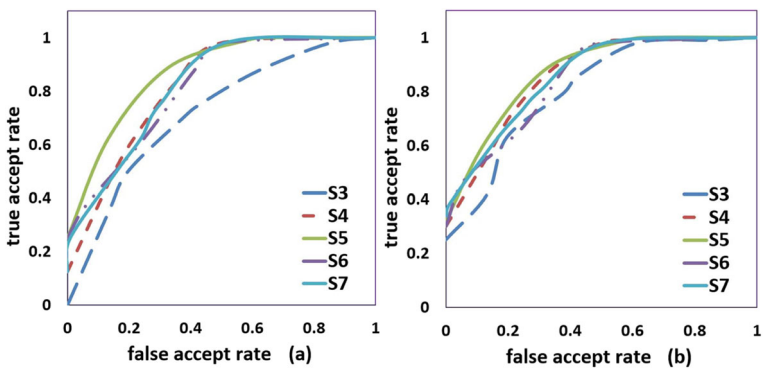

Fig. 12 ROC result with different numbers of stripes. **a**: Texas3D, **b**: Gavab

Table 2 Comparing facial average searching speed in hierarchical structures with different methods in Gavab

	Gavab		Texas3D	
Method	Ast	Ast-HS	Ast	Ast-HS
3DWW	15.5s	3.2s	12.1s	2.8s
SRV	68.4s	12.3s	38.4s	10.3s
D2DWW	12.4s	2.7s	9.3s	2.1s

Ast: average searching time without facial structure. Ast-HS: average searching time in hierarchical structure

set. In Fig. 13, we show the structure's search improvement using different methods on different test sets. Using the facial hierarchical structure, the search process in a facial database with more than 200 samples can achieve an average of a 400% speed improvement rate.

5.3 Facial hierarchical structure for facial classification accuracy

We use three parts to evaluate facial classification accuracy in the structure. First, we compare measurement results from different facial measurement methods. The facial hierarchical structure is based on the facial measurement method. Several characteristics, such as facial expressions and triangulation robustness in structure, are provided by the facial measurement method. Second, we use different facial measurement methods to construct facial hierarchical structures. We compare the facial classification accuracy from different structures. The facial search process in the structures can be regarded as the facial classification task. The input face should be classified to certain nodes after searching the structure, such as in Fig. 9. The facial search process should be robust to different facial expressions and different triangulation accuracy. Third, we provide an "one to many" scheme in our facial hierarchical structure construction. We compare the performance between the "one

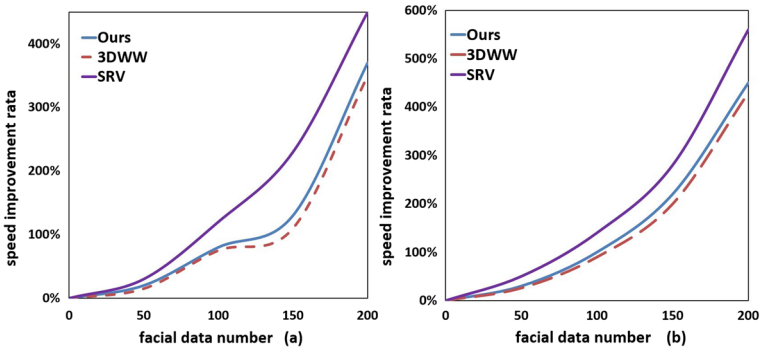

Fig. 13 Different measurement methods are used to construct different facial structures. The facial search speed improvements are obvious in the facial structures when the facial test sets are larger. We show the speed improvement rate using different facial structures to facial test sets from Gavab (**a**) and Texas3D (**b**). The search process based on the SRV can achieve obvious improvements. The reason is the measurement by the SRV is slower than other methods. The facial hierarchical structure reduces the measurement times for facial searching, and then the speed improvement rate is more obvious for the SRV

Table 3 3D facial measure for several faces from Gavab with different methods

Faces	Method	Caral (frontal1)	Cara1 (risa)	Cara2 (frontal1)	Cara2 (risa)	Cara3 (frontal1)	Cara3 (risa)
caral(frontal1)	3DWW	0	0.3046	0.1474	0.1696	0.2429	0.2337
	SRV	0	0.5642	0.5749	0.6886	0.6464	0.5126
	D2DWW	0	0.037	0.188	0.168	0.174	0.178
cara1(risa)	3DWW	0.3046	0	0.3703	0.3231	0.3107	0.3077
	SRV	0.642	0	0.5650	0.6070	0.7472	0.6487
	D2DWW	0.037	0	0.183	0.161	0.159	0.154
cara2(frontal1)	3DWW	0.1474	0.3703	0	0.08611	0.2247	0.2207
	SRV	0.5749	0.5650	0	0.6304	0.6919	0.6418
	D2DWW	0.188	0.183	0	0.052	0.173	0.176
cara2(risa)	3DWW	0.1696	0.3231	0.08611	0	0.2324	0.2264
	SRV	0.6886	0.6070	0.6304	0	0.7314	0.7304
	D2DWW	0.168	0.161	0.052	0	0.186	0.173
cara3(frontal1)	3DWW	0.2429	0.3107	0.2247	0.2324	0	0.03826
	SRV	0.6464	0.7472	0.6919	0.7467	0	0.6719
	D2DWW	0.174	0.159	0.173	0.186	0	0.04
cara3(risa)	3DWW	0.2337	0.077	0.2207	0.2264	0.03826	0
	SRV	0.5126	0.6487	0.6418	0.7468	0.6719	0
	D2DWW	0.178	0.154	0.176	0.173	0.04	0

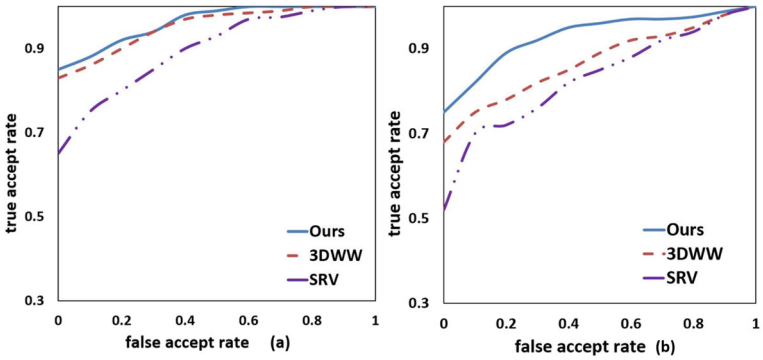

Fig. 14 Comparing different facial structure using different methods. **a** ROC for Gavab, **b** ROC for Texas3D

to many" scheme and the original one. Finally, we re-sample facial data by different triangulation accuracy to build a test facial set, which is used to demonstrate the triangulation robustness of our facial hierarchical structure.

We show the measure instances in Table 3. The instances of facial data are chosen in Gavab. We choose the two samples (frontal1 and risa) from three people. In the R3 space, the 3D facial data is dependent on a coordinate system. The results are affected by the head poses in the 3DWW. For SRV, the triangulation's precision is affected by the performance of the facial similarity measurement. The 3D face with coarse triangulation produces noise for iso-geodesic curves. Our surface measurement results have similar values for one person with different facial expressions. For each row, we notice more small value between two faces. The blue one is the wrong value. The blue one means the faces from different people are smaller than the faces from same one. The red one is true value. It means the faces from the same person are more similar. In Table 3, our method can achieve more red values.

Facial data from one person is considered to be a facial class. The search process inputs target facial data and uses it to compare every mean facial data in the node of a structure. Every facial data in the structure has a parent node. The facial data from one person should have the same parent node. We construct the facial structure using 61 faces without expressions from 61 people from Gavab and build a test set from other facial data to test the

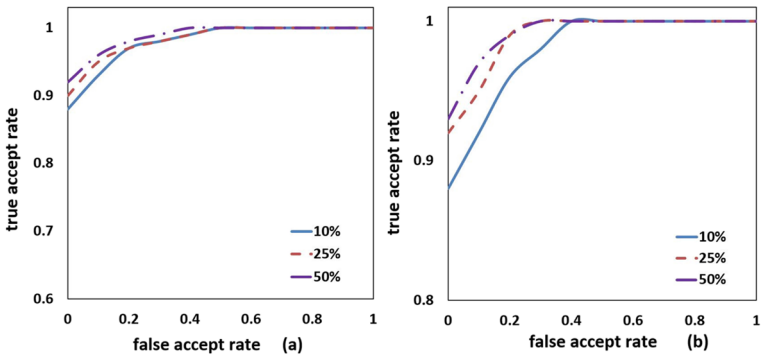

Fig. 15 Comparing the faces with different accuracy in our facial structure. **a** ROC for Gavab, **b** ROC for Texas3D

accuracy of different structures. We also construct the facial structure using 100 faces without expressions from 100 people from Texas3D and process the same test. We compute the ROC results by different facial structures in Fig. 14.

Our facial hierarchical structure is robust to triangular meshes with different accuracies. We construct two facial data sets, 61 faces from Gavab and 100 faces from Texas3D with different triangulation accuracy (10%, 25% and 50% of original meshes). Using this set as the input data in the facial hierarchical structure, we achieve the facial classification results. In Fig. 15, we show the facial classification ROC results of the facial set. The results show that our facial hierarchical structure is robust to meshes with differing triangulation accuracy.

In summary, the D2DWW is robust to facial expressions, head poses and different accurate of facial triangular meshes. Based on the D2DWW, the facial hierarchical structure can be constructed and the face searching speed is improved obviously. The SRV based methods [15, 25] provide a facial measure framework which is robust to facial expressions and head poses. However, the iso-geodesic curves for elastic shape analysis are sensitive to different accurate triangular meshes. The time cost of the methods is more than other methods. The iso-geodesic curves [1] and 3DWW based methods [5] propose a facial measure framework which is robust to different facial expressions and not sensitive to triangular meshes. However, the methods are affected by different head poses. Our facial hierarchical structure construction framework solves the problems from such methods, which provides a practical solution for 3D face similarity measure and 3D facial data organization.

6 Conclusions

We propose a novel 3D facial hierarchical structure construction framework for facial similarity measure and facial data organization. The framework includes facial similarity measure based on 2DFADR and facial hierarchical structure construction. The 2DFADR is a 2D facial reflection from a 3D facial surface with area distortion information. The 2DFADR preserves the geometric information from a 3D facial surface and removes the influence of head pose. This framework provides a convenient, regular facial representation for 3D facial data. Based on the 2DFADR, we provide the facial similarity measurement method: D2DWW. The D2DWW is robust to facial expressions and different accuracy of triangulation meshes. This method is mathematically metric to the 2DFADR. Using the measurement results, we achieve the distance matrix from a large facial database. The Facial Hierarchical Structure is constructed based on the matrix. The facial data in the facial hierarchical structure is effectively organized. For the facial data search process, the structure can improve the search speed and be robust to facial expressions and the accuracy of triangulation meshes. In future works, we will attempt to study more visually geometric features for 3D face similarity measurements and improve the facial structure accuracy. We also require a more general solution to process the complex topological structures of faces.

Acknowledgements This research was partially supported by the National Key Cooperation between the BRICS Program of China (No.2017YE0100500), National Key R&D Program of China (No. 2017YFB1002600, No.2017YFB1402105) and Beijing Natural Science Foundation of China (No.4172033). We thank the face database (Gavab and Texas3D) and method's code provider in github. We also thank the provider of geodesic path tools (GeodesicLib; http://www.cs.technion.ac.il/vitus/papers/GeodesicLib.zip).

References

1. Ahdid R, Safi S, Manaut B (2015) Three Dimensional Face Surfaces Analysis using Geodesic Distance. J Comput Sci Appl [J] 3:67–72
2. Antipov G, Baccouche M, Berrani SA, Dugelay JL (2016) Apparent age estimation from face images combining general and Children-Specialized deep learning models. IEEE Conference on Computer Vision and Pattern Recognition Workshops [C] 1:801–809
3. Ballihi L, Amor BB, Daoudi M, Srivastava A (2012) Geometric Based 3D Facial Gender Classifi-CatioN. In: International Symposium on Communications Control and Signal Processing [J], pp 1–5. https://doi.org/10.1109/ISCCSP.2012.6217828
4. Berretti S, Bimbo D, Vicario E (2003) Weighted walkthroughs between extended entities for retrieval by spatial arrangement. IEEE Trans Multimed [J] 5(1):52–70
5. Berretti S, Bimbo A, Pala P (2010) 3D face recognition using iso-geodesic stripes. IEEE Trans Pattern Anal Mach Intell [J] 32(12):2162–2177
6. Berretti S, Bimbo AD, Pala P (2012) Distinguishing facial features for ethnicity-based 3d face recognition. ACM Trans Intell Syst Technol [J] 3(3):45
7. Blanz V, Vetter T (1999) A morphable model for the synthesis of 3D faces. SIGGRAPH '99 [C]:187–194. https://doi.org/10.1145/311535.311556
8. Blanz V, Vetter T (2003) Face recognition based on fitting a 3D morphable model. IEEE Trans Pattern Anal Mach Intell (IEEE TPAMI) [J] 25(9):1063–1074
9. Bronstein AM, Bronstein MM, Kimmel R (2005) Three dimensional face recognition. Int J Comput Vis [J] 64(1):5–30
10. Bronstein AM, Bronstein MM, Kimmel R (2006) Expression-invariant representations of faces. IEEE Trans Image Process [J] 16(1):188–197
11. Cao C, Weng Y, Zhou S, Tong Y, Zhou K (2014) Facewarehouse: A 3D Facial Expression Database for Visual Computing. IEEE Trans Vis Comput Graph [J] 20(3):413–425
12. Choi SE, Lee YJ, Lee SJ, Kang RP, Kim J (2011) Age estimation using a hierarchical classifier based on global and local facial features. Pattern Recogn [J] 44(6):1262–1281
13. Coates A, Ng AY (2012) Learning Feature Representations with K-means. Lect Notes Comput Sci [J]. 7700:561–580
14. Desbrun M, Meyer M, Alliez P (2002) Intrinsic parameterizations of surface meshes. Eurographics [C] 21(3):209–218
15. Drira H, Amor B, Srivastava A, Daoudi M (2010) A riemannian analysis of 3D nose shapes for partial human biometrics. IEEE International Conference on Computer Vision [C] 30(2):2050–2057
16. Fakir M, Ahdid R, Taifi K et al (2015) Two-Dimensional Face recognition methods comparing with a riemannian analysis of Iso-Geodesic curves. J Electron Commer Organ [J] 13(3):15–35
17. Feng LZ, Ou TX (2004) Bayesian face recognition using support vector machine and face clustering. IEEE Comput Soc Conf Comput Vis Pattern Recogn [C] 2:374–380
18. Frey BJ, Dueck D (2007) Clustering by passing messages between data points. Science [J] 315(5814):972–6
19. Ghahari A, Fatmehsari YR, Zoroofi RA (2009) A novel Clustering-Based feature extraction method for an automatic facial expression analysis system. International Conference on Intelligent Information Hiding and Multimedia Signal Processing [C]:1314–1317. https://doi.org/10.1109/IIH-MSP.2009.38
20. Gilani SZ, Shafait F, Mian A (2015) Shape-based Automatic Detection of a Large Number of 3D Facial Landmarks. IEEE Conf Comput Vis Pattern Recognit (CVPR) [C] 07:4639–4648
21. Horng WB, Lee CP, Chen CW (2001) Classification of age groups based on facial features. Tamkang J Sci Eng [J] 4(4):183–192
22. Jahanbin S, Choi H, Liu Y et al (2008) Three dimensional face recognition using Iso-Geodesic and Iso-Depth curves. IEEE international conference on biometrics: Theory. Applications and Systems[C]:1–6. https://doi.org/10.1109/BTAS.2008.4699378
23. Jahanbin S, Jahanbin R, Bovik AC et al (2013) Passive three dimensional face recognition using Iso-Geodesic contours and procrustes analysis. Int J Comput Vis [J] 105(1):87–108
24. Jermyn IH, Kurtek S, Klassen SE, Srivastava A (2012) Elastic shape matching of parameterized surfaces using square root normal fields. European conference on computer vision [C]. pp 804–17
25. Kurtek S, Drira H (2015) A comprehensive statistical framework for elastic shape analysis of 3D faces, vol 51
26. Lopes AT, Aguiar ED, Souza AFD, Oliveira-Santos T (2017) Facial expression recognition with Convolutional Neural Networks: Coping with few data and the training sample order. Pattern Recogn [J] 61:610–628

27. Luciano L, Hamza AB (2017) Deep learning with geodesic moments for 3D shape classification [J]. Pattern Recognition Letters
28. Lyons MJ, Budynek J, Akamatsu S (1999) Automatic classification of single facial images. IEEE Trans Pattern Anal Mach Intell [J] 21(12):1357–1362
29. Masoumi M, Hamza AB (2017) Spectral shape classification: A deep learning approach[J]. J Vis Commun Image Represent 43:198–211
30. Mühling M, Korfhage N, Müller E et al (2017) Deep learning for content-based video retrieval in film and television production [J]. Multimed Tools Appl [J] 76(2):1–26
31. Otto C, Wang D, Jain A (2016) Clustering millions of faces by identity [J]. IEEE Trans Pattern Anal Mach Intell [J]. 40(2):1–1
32. Park HS, Jun CH (2009) A simple and fast algorithm for K-medoids clustering. Expert Syst Appl [J] 36(2):3336–3341
33. Paysan P, Knothe R, Amberg B, Romdhani S, Vetter T (2009) A 3D face model for pose and illumination invariant face recognition. Advanced Video and Signal Based Surveillance [J]:296–301. https://doi.org/10.1109/AVSS.2009.58
34. Pickup D, Sun X, Rosin PL et al (2016) Shape Retrieval of Non-rigid 3D Human Models[J]. Int J Comput Vis 120(2):169–193
35. Shan SL, Khalil-Hani M, Radzi SA, Bakhteri R (2016) Gender classification: a convolutional neural network approach. Turkish J Electr Eng Comput Sci [J] 24(3):1248–1264
36. Srivastava A, Klassen E, Joshi SH, Jermyn IH (2010) Shape analysis of elastic curves in euclidean spaces. IEEE Trans Pattern Anal Mach Intell (IEEE TPAMI) [J] 33(7):1415–1428
37. Surazhsky V, Surazhsky T, Kirsanov D et al (2005) Fast exact and approximate geodesics on meshes[J]. Acm Trans Graph 24(3):553–560
38. Wu J, Smith WAP, Hancock ER (2007) Gender Classification using Shape from Shading. Proceedings of the British Machine Vision Conference [C]:50.1–50.10. https://doi.org/10.5244/C.21.50
39. Xia J, He Y, Quynh D, Chen X, Hoi CH (2010) Modeling 3D Facial Expressions using Geometry Videos. Proceedings of ACM Multimedia (MM '10) [C] 22(1):591–600
40. Xia J, Quynh D, He Y, Chen X, Hoi SCH (2012) Modeling and compressing 3D facial expressions using geometry videos. IEEE Trans Circ Syst Video Technol [J] 22(1):77–90
41. Yu D, Wu XJ (2017) 2DPCANEt: a deep leaning network for face recognition [J]. Multimed Tools Appl [J] 4:1–16
42. Zeng W, Hua J, Gu X (2009) Symmetric Conformal Mapping for Surface Matching and Registration. Int J CAD/CAM (IJCC) [J] 9(1):103–109
43. Zeng W, Samaras D, Gu X (2010) Ricci flow for 3D shape analysis. IEEE Trans Pattern Anal Mach Intell (IEEE TPAMI) [J] 32(4):662–677
44. Zeng W, Gu X (2011) Conformal geometric methods in computer vision. IEEE CEWIT conference (CEWIT'11) [C]

Chenlei Lv is studying for PhD degree in College of information science and technology, Beijing Normal University (BNU). His reasearch interests include computer vision, 3D biometrics, computer graphic, discrete differential geometry and confromal geometric.

Zhongke Wu is Full Professor in College of information science and technology, Beijing Normal University (BNU), China. Currently he is the member of Steering Committee for Professional Teaching of Animation, digital media in Colleges and universities of Ministry of Education, China and member of CCF CAD and Graphics and CCF Human Computer Interaction. He led and took part in various research and development projects in computer graphics and related areas. Prof.WU's current research interests include computer graphics, animation virtual reality, geometric modeling, volume graphics and medical imaging.

Xingce Wang has achieved the new title (Full Professor) recently in College of Information Science and Technology, Beijing Normal University, PR China. She is major in the 3D modeling and 3D visualization. Her current research interests include computer graphic, medical imaging, artificial intelligence and Machine learning.

Mingquan Zhou is the super visor of doctor candidates and the dean in College of Information Science and Technology, Beijing Normal University, PR China. His current research interests include computer graphics, and 3Dvisualization.